The Korean Journal of Ceramics, 4 [2] 114 - 121 (1998)

Partial Conductivity of YSZ Doped with 10 mol% TiO_2

Kiyoshi Kobayashi, Yukiharu Kai, Shu Yamaguchi, Tsuyoshi Kawashima* and Yoshiaki Iguchi

Department of Material Science and Engineering, Nagoya Institute of Technology
Gokiso-cho, Showa-ku, Nagoya 466, Japan
**Fundamental Technology Research Laboratory, Tokyo Gas Co., Ltd*
Shibaura 1-16-25, Minato-ku, Tokyo 105, Japan
(Received October 2, 1997)

Using Hebb-Wagner's asymmetric cell, partial conductivities of holes and electrons in yttria stabilized zirconia doped with 10 mol% TiO_2 have been estimated by a dc polarization measurement. The current interruption method and ac impedance measurements have been also made to evaluate the ionic conductivity and to examine the consistency of the partial conductivities Partial conductivities of electrons (σ_n) and holes (σ_p) were found to be proportional to -1/4 and 1/4 power of partial pressure of oxygen gas, respectively, except for σ_n at reducing conditions. In comparison with 5 mol% doped YSZ, σ_n was found to increase with the increase of TiO_2 concentration, but σ_p stayed at almost a constant value.

Key words : Yttria stabilized zirconia, Titania, Electronic conductivity, Dc polarization, Mixed conductor, Phase stability

I. Introduction

Mixed electronic and oxide ion conductors have attracted attention for the application as anode materials in solid oxide fuel cell applications and other electrochemical devices for energy conversion systems. Among various candidate materials, attention has been focused on titania-doped YSZ (TD-YSZ) because of the chemical stability and materials compatibility with YSZ as well as a novel concept of single-component oxide fuel cell.[1] Various experimental approaches have been made not only for applications but also for the better understandings of the mechanism and the effect of the dopant on its electronic transport properties of this unique material. Althogh total conductivity and partial conductivities of holes and electrons for TD-YSZ have been separately measured,[2-5] the consistency between these conductivities has not been confirmed yet. In addition, phase stability of TD-YSZ has never been paid attention during the course of the experiments. The authors have been extensively examined the phase stability of solgel derived TD-YSZ solid solution,[6] total conductivity measurements in a wide range of composition,[7] and partial conductivity measurements by dc polarization method. In this study, the partial and total conductivity of yttria stabilized zirconia doped with 10 mol% TiO_2 (10TD-YSZ) have been measured by both dc polarization and ac impedance methods, and the stability during long term operation at high temperatures is examined.

II. Experimental

The sample used in the present study was a ceramics tube of closed one end with a rim around the open end. The sample composition was 82 mol% ZrO_2 - 8 mol% Y_2O_3 - 10 mol% TiO_2 ($Y_{0.148}Zr_{0.759}Ti_{0.093}O_{1.926}$: denoted as 10TD-YSZ hereinafter), which was prepared by a conventional solid state reaction and sintering process at 1923 K. The tube was specially manufactured and supplied for the present study by Tosoh Co. Ltd. The preparatory method and the dimensions of the sample tube were the same as those in the previous report on the dc polarization measurements of 5 mol% TiO_2 doped YSZ (STD-YSZ).[5] Similarly to the previous report, platinum paste (No OP07, Tanaka Kikinzoku Kougyou, K.K, Japan) was painted on both inside and outside of the wall and fired at 1273 K for 10 h in air. The procedure was repeated three times. Resultant areas of inner and outer electrodes were 28.8 and 23.0 cm^2, respectively.

The design of the dc polarization cell and the experimental procedures based on the Hebb-Wagner's asymmetric cell, were almost identical to the previous report. The measurements have been mainly performed at 1073, 1123, 1173, 1223 and 1273 K under the oxygen fugacity at the reversible elctrode, $p_{O_2}^{rev}$, between 10^{-2} and 1, using the gas mixtures of various ratio of O_2 and Ar. The oxygen fugacity is defined as $p_{O_2}=(P_{O_2}/Pa)/(P^{\ominus}/Pa)$, where $P^{\ominus}$ is the standard pressure of 1.013×10^5 Pa. For additional low $p_{O_2}^{rev}$ measurements between 10^{-12}-10^{-14}, CO+CO_2 gas mixture was used. The values of $p_{O_2}^{rev}$ were

monitored by a zirconia oxygen sensor placed near the sample during the measurements. The potentiostatic dc polarization was made by applying voltage ranging from 0.25 and 1.4 V, and the value of current, i_{ext}, was measured by a digital multimeter (model 3497 A, Hewlett Packard) after the steady state was achieved.

A current interruption technique was also employed for the determination of the transference number of oxide ions during the dc polarization measurements, where the current was interrupted after the steady state was achieved and the decay of the open circuit voltage was measured with the settling time of 15 or 30 ms.

Total conductivity, σ_t, was measured by a two-probe ac impedance method for block-shaped sample with the dimension of $4.7\times1.3\times1.0$ mm which was cut off from the tubular sample after the polarization cell was cooled to room temperature. The sample was again heated at 1873 K for 10 h in order to restore the initial state because of possible phase separation during the long term polarization measurements. The measurements were made using frequency response analyzer (S-5720B, NF Electronic Inst.) between 1 Hz and 100 kHz with the amplitude of 100 mV. Gas mixtures of O_2+Ar or H_2+Ar+CO_2 were used to maintain the oxygen fugacity in ac impedance measurements, monitored by zirconia sensor placed near the sample.

The polarization measurements were made after the sample had been heated at 1273 K with applying voltage of 1.0 V across the cell for 40 days to examine the phase stability of 10TD-YSZ. Total annealing period was 486 days since the measurements were started, and the sample was cooled from 1273 K to room temperature at 8 K/s in a furnace with applying voltage of 1.0 V. A part of the sample was crushed into powder, and X-ray diffraction (XRD) pattern of the sample was obtained at room temperature.

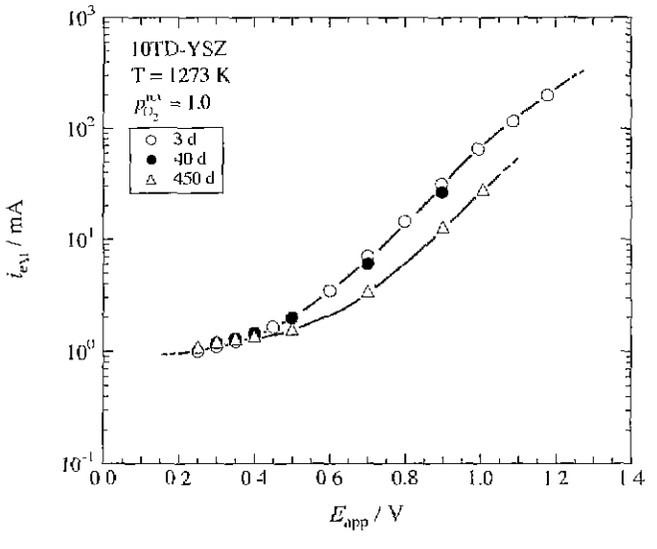

Fig. 1. The relationships between i_{ext} and E_{app} for the same sample with the different annealing period of 3, 40 and 450 d.

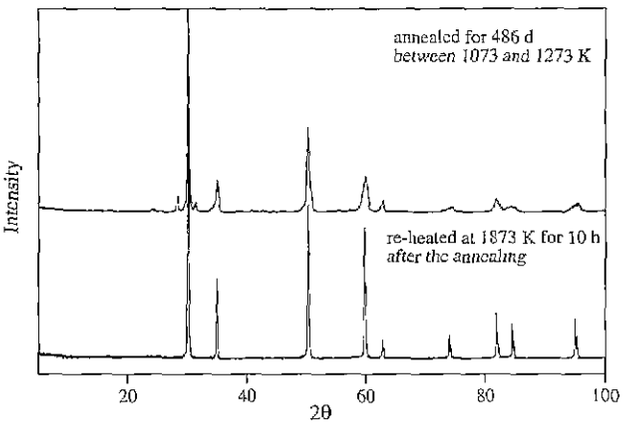

Fig. 2. X-ray powder diffraction patterns 10TD-YSZ obtained (a) after the 486 days annealing and (b) the sample heated again at 1873 K for 10 h after the annealing (a).

III. Results

1. Phase stability

The polarization curves with the different annealing period are shown in Fig. 1. The values of the steady state current shifted by the prolongation of annealing period. The change in the polarization was particularly evident after 40 days. Fig. 2 shows XRD pattern for 10TD-YSZ heated between 1073 and 1273 K for 486 days. The pattern clearly shows the existence of two phases of cubic fluorite and monoclinic baddeleyite structure. A part of the sample was subjected to heat treatment again at 1873 K for 10 h after the polarization measurements, and the XRD pattern was found to consist of the peaks of cubic fluorite phase. As discussed in the previous report in detail,[8] the monoclinic phase was transformed from the tetragonal phase during cooling or pulverizing process. Therefore, it is concluded that 10TD-YSZ decomposed from oversaturated cubic fluorite phase, which was stable at the sintering temperature, into cubic and tetragonal phases due to large temperature dependence of the solid solubility of TiO_2. All the results on the electrochemical measurements employed in the present study was collected within 40 days.

2. Dc polarization measurements

Typical results of the polarization measurement at 1273, 1173 and 1073 K under the oxygen fugacity at the reversible electrode, $p_{O_2}^{lev}$=1.0 are shown in Fig. 3. Although the cell was designed to be a four probe one, a single lead wire instead of two lead wires in the previous study, was used in the interior part of the cell. Therefore the small correction for platinum resisitivity on the measured voltage was made using the literature data.[8] The rapid increase of i_{ext} with increasing the E_{app} are found in the regime from 0.4 to 1.4 V. The magnitude of the i_{ext} values for 10TD-YSZ are found to be about 10 times larger than the values for 5TD-YSZ[5] in the range

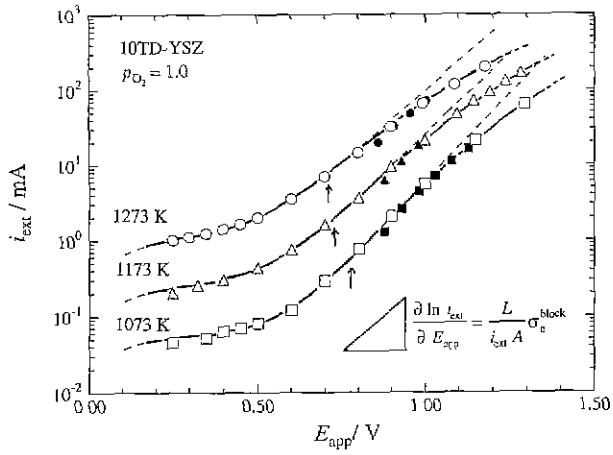

Fig. 3. The relationships between steady state current, i_{ext} and applied voltage, E_{app} by the dc polarization measurements for 10TD-YSZ equilibrated at 1273, 1173 and 1073 K under log $p_{O_2}^{rev}$=0. The polarization results under reducing condition log $p_{O_2}^{rev}$=-11.1 at 1273 K, log $p_{O_2}^{rev}$=-12.4 at 1173 K and log $p_{O_2}^{rev}$=-14.7 at 1073 K are also plotted by closed symbols. Dashed curves indicate the i_{ext}-E_{app} relationship in the case of $\sigma_n \propto p_{O_2}^{-1/4}$.

of E_{app} from 0.6 to 1.4 V.

The total electronic conductivity, $\sigma_e^{block}=\sigma_n^{block}+\sigma_p^{block}$ at $p_{O_2}^{block}$ can be calculated by the following equation,[9]

$$\sigma_e^{block}=\frac{L}{A}\frac{\partial i_{ext}}{\partial E_{app}}=\frac{L}{A}\cdot i_{ext}\cdot\frac{\partial \ln i_{ext}}{\partial E_{app}}, \quad (1)$$

where A and L are the electrode area and thickness of the sample. σ_e^{block} values are calculated in the same manner as in the previous report,[5] and the results are plotted by solid marks in Fig. 4. All the plots at each

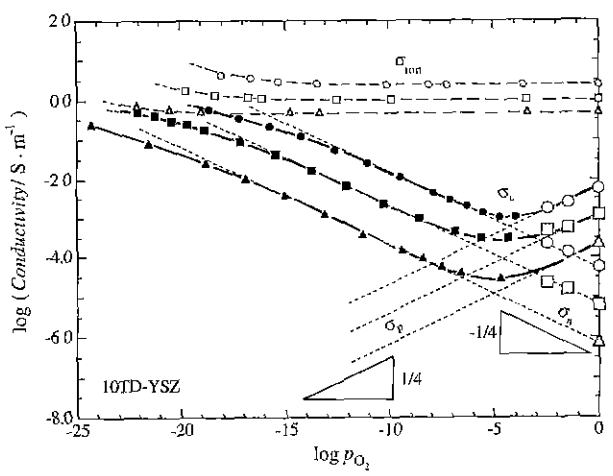

Fig. 4. The relationships of σ_e (closed symbol) determined by the slope of polarization curves in Fig. 3, σ^*_n and σ^*_p determined from the Wagner's method (open symbols), σ_t (small open symbols with broken curves) measured by ac method. Solid curves indicate σ_e calculated ones from σ_n and σ_p by the slope and Wagner's method. The dotted lines shows $p_{O_2}^{-1/4}$ adn $p_{O_2}^{1/4}$ dependencies of σ_n and σ_p, predicted from the defect models.

temperature fall on the straight line, proportional to -1/4 power of p_{O_2} at higher p_{O_2} region in n-type domain, but exhibits upward convex at reducing conditions, which is more apparent than 5TD-YSZ. The extent of the deviations becomes more severe at high temperature. Due to the contribution of hole conductivity, which is suggested to be proportional to 1/4 power of p_{O_2} by the defect model discussed later, σ_e^{block} shows positive deviation from -1/4 relationship p_{O_2}>10^{-7}-10^{-10}.

The Wagner's analysis was also made using eq'n (2),[10] where partial conductivities of electrons, σ_n, and holes, σ_p, are assumed to be proportional to -1/4 nd +1/4 powers of p_{O_2}

$$i_{ext}=\frac{RTA}{FL}\left\{\sigma^*_n(\exp[u]-1)+\sigma^*_p(1-\exp[-u])\right\} \quad (2)$$

T, R, F, σ^*_n and σ^*_p are absolute temperature, gas constant, Faraday constant, and conductivities of electrons and holes in equilibrium with $p_{O_2}^{rev}$ respectively, and $u=E_{app}F/RT$. Rewriting eq'n (2), the plots of $i_{ext}/(\exp[u]-1)$ against $(1-\exp[-u])/(\exp[u]-1)$ and $i_{ext}/(1-\exp[-u])$ against $(\exp[u]-1)/(1-\exp[-u])$ show linear relationships and each set of σ_n^* and σ_p^* values can be obtained separately from the slopes and intercepts. Pairs of the plots using the measured data at 1273 K at log $p_{O_2}^{rev}$=0, -1.5 and 2.4, 1173 K at log $p_{O_2}^{rev}$=0 and 1073 K at log $p_{O_2}^{rev}$=0 are shown in Fig. 5 (a)-(b), (c)-(d) and (e)-(f), respectively. All of the plots at log $p_{O_2}^{rev}$=0 show linear relationships, except for the regime of E_{app}>450 mV as illustrated in Fig. 5. (a)-(b). Pairs of the values for σ_n^* and σ_p^* calculated from both of the plots show good agreement with each other, if the data below E_{app}>450 mV are used for the calculation. The σ_n^* and σ_p^* values are shown in Fig. 4 by open marks. Excellent agreement between σ_n^* and σ_n^{block} extrapolated from lower p_{O_2} is observed. σ_e estimated from σ_n and σ_p by the both methods is illustrated by solid curves in Fig. 4, indicating consistency between both methods at high p_{O_2} regime.

3. Current interruption and ac impedance measurements

A typical variation of voltage with time is shown in Fig. 6 when the cell circuit is open after the steady state is attained. Values of E_{app} for the steady state condition and E_{app} just after the abrupt change in the voltage across the cell was recorded. The correlation of the resistivity of Pt due to the incomplete set-up for the interior lead wire was made for the values of E_{app} by the same manner as mentioned above. Fig. 7 depicts the relation between E_{app} and E_{apon} measured at fixed $p_{O_2}^{rev}$ at reversible electrode of 1.0. The transference number of ions at p_{O_2}, which corresponds to E_{app} through the equation,

$$4FE_{app}=-RT\ln(p_{O_2}^{block}/p_{O_2}^{rev})=-(\mu_{O_2}^{block}/\mu_{O_2}^{rev}), \quad (3)$$

can be evaluated from the slope of each E_{app} using the transference numbers of ion, t_{ion}, as,

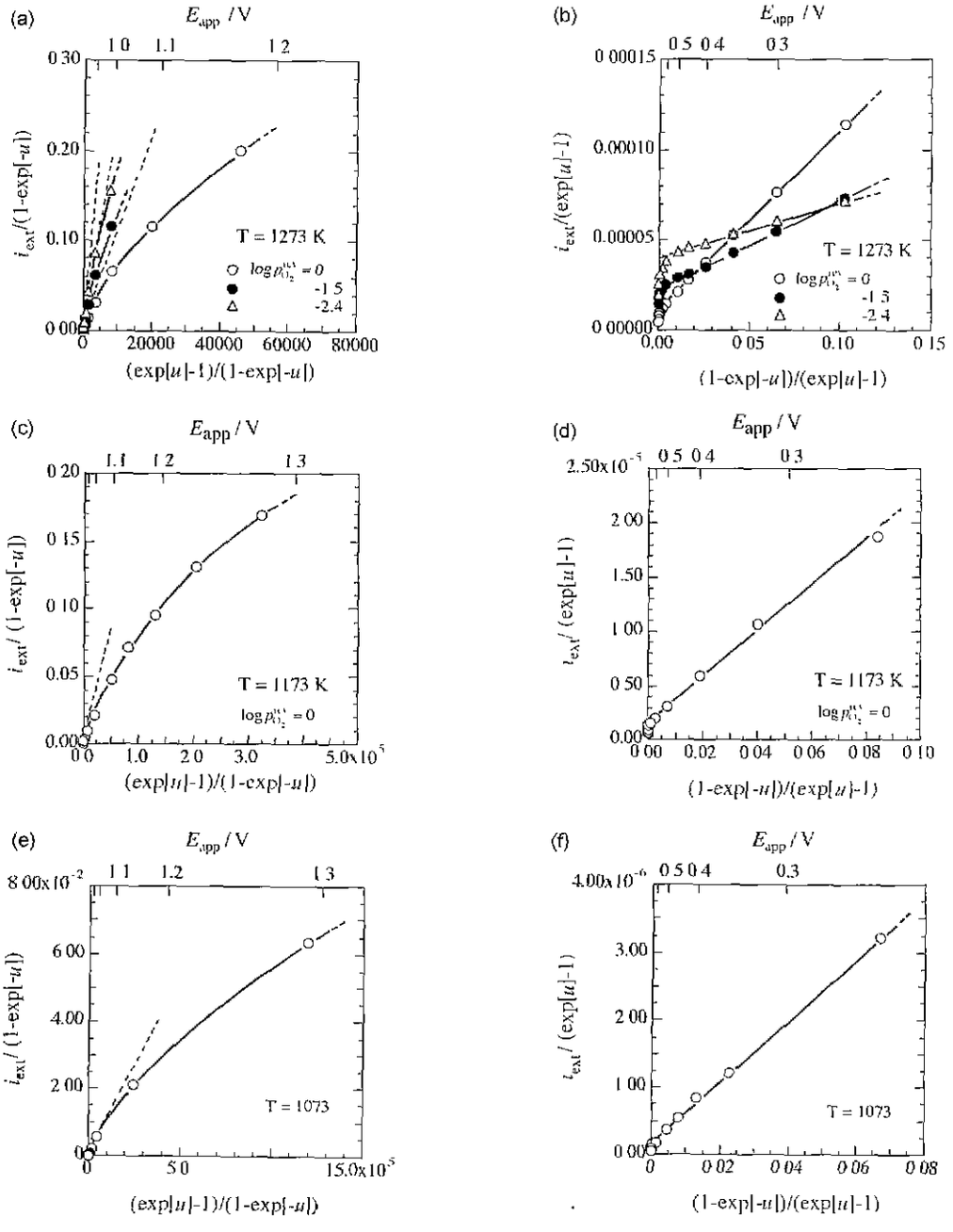

Fig. 5. Plots of $i_{ext}/(\exp[u]-1)$ against $(1-\exp[-u])/(\exp[u]-1)$ ((a), (c), (e)) and $i_{ext}/(1-\exp[-u])$ against $(\exp[u]-1)/(1-\exp[-u])$ ((b), (d), (f)) at 1273 K and $\log p_{O_2}=0$, respectively and $u=E_{app}F/RT$.

$$\frac{dE_{open}}{dE_{app}} = t_{ion}, \tag{4}$$

sinec E_{open} is expressed as, $-4FE_{open} = \int_{p_{O_2}=p_{O2}^{new}}^{p_{O_2}=p_{O2}^{block}} t_{ion} d(RT \ln p_{O_2})$.

Resultant t_{ion} are plotted in Fig. 8.

The total conductivity measured by an ac impedance method are plotted in Fig. 4. Since t_{ion} decreases with the decrease of p_{O_2}, the complex impedance plot changes from a typical semi-circle trace for ionic conductors to a non-dispersion one which tend to focus on a single point irrespective to frequencies.

IV. Discussions

1. Defect model

The predominant defect in TiO_2-doped YSZ is considered to be almost identical to the normal YSZ, where the extrinsic defect of oxygen vacancy forms by the charge compensation of doped Y^{3+} substituted for $(Zr/Ti)^{4+}$ ions due to the electrical neutrality condition. Using Kröger-Vink notation, the defect model is

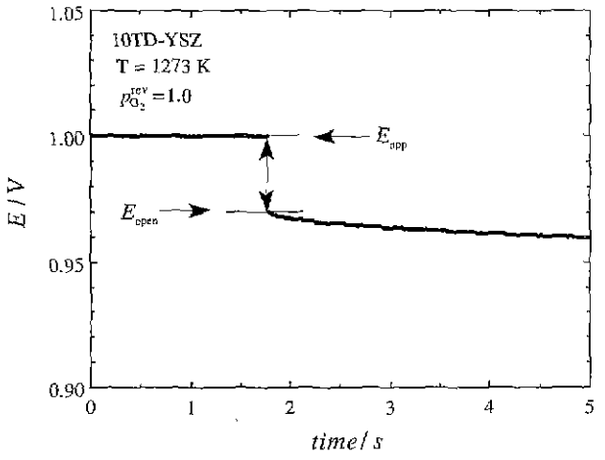

Fig. 6. An example of the current interruption measurements: V ariation of emf of the cell with time.

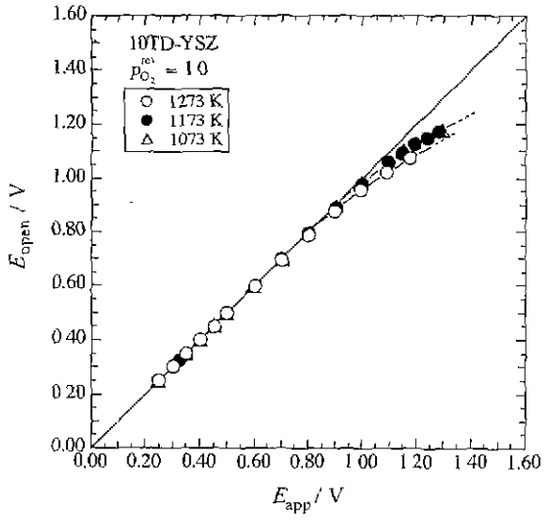

Fig. 7. *The relations between E_{app} and E_{open} at 1073, 1173, and 1273 K measured by the current interruption method.*

summarized as follows : The equilibrium constant K_{V_O} for the formation of oxygen vacancy (Vö),

$$O_O^x = \frac{1}{2}O_2 + V_{\ddot{O}}^{\cdot\cdot} + 2e', \tag{A}$$

can be written as,

$$K_{V_O} = [V_{\ddot{O}}^{\cdot\cdot}]\, n^2\, p_{O_2}^{1/2}, \tag{5}$$

where [Vö] and n are the concentrations of Vö an free electrons (e'), respectively. The intrinsic ionization process of electrons and holes (h˙),

$$0 = e' + h^{\cdot} \tag{B}$$

yields the following relationship using concentrations of electrons, holes (p), and the equilibrium constant for the reaction (B), K_i, as

$$K_i = n \cdot p. \tag{6}$$

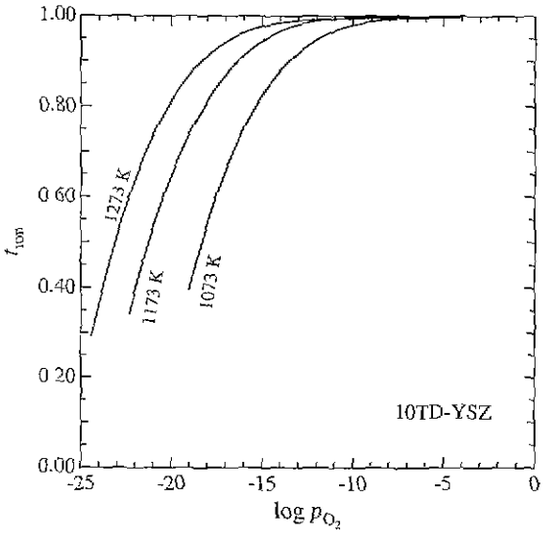

Fig. 8. Transference number of ions, t_{ion}, calculated from the slope of the curves in Fig. 7.

A part of free electrons may be trapped by the Ti ions through the reaction,

$$Ti_{Zr}^x + e' = Ti'_{Zr}, \tag{C}$$

where Ti_{Zr}^x and Ti'_{Zr} are neutral and singly negatively-charged titanium ions on Zr sites. Equilibrium constant for the formation of Ti'_{Zr}, K_{Ti}, is given by the following equation,

$$K_{Ti} = \frac{[Ti'_{Zr}]}{[Ti_{Zr}^x]n}, \tag{7}$$

where $[Ti'_{Zr}]$ and $[Ti_{Zr}^x]$ are the concentration of Ti_{Zr}^x and Ti'_{Zr}, respectively.

The overall charge neutrality condition can be expressed as

$$2[V_{\ddot{O}}^{\cdot\cdot}] + p = [Y'_{Zr}] + n + [Ti'_{Zr}], \tag{8}$$

where $[Y'_{Zr}]$ is the concentration of singly negatively-charged yttrium ions on Zr sites. Because Ti'_{Zr} formation can be neglected at high p_{O_2} regime, i.e. $[Ti_{Zr}^x] >> [Ti'_{Zr}]$, the assumption on the charge neutrality condition that $2[V_{\ddot{O}}^{\cdot\cdot}] \approx [Y'_{Zr}] >> n$, p leads to the following equations.

$$n = \left(\frac{2 \cdot K_{V_O}}{[Y'_{Zr}]}\right)^{1/2} p_{O_2}^{-1/4}, \text{ and} \tag{9}$$

$$P = K_i \cdot \left(\frac{[Y'_{Zr}]}{2 \cdot K_{V_O}}\right)^{1/2} \cdot p_{O_2}^{1/4}. \tag{10}$$

At lower p_{O_2} regime, it is necessary to evaluate Ti'_{Zr} fraction in the total titanium ion concentration for the detailed discussion on the partial conductivity at reducing conditions. *EPR*[11] and coloration[12] measurements have indicated that $[Ti'_{Zr}]$ is much lower than $[Ti_{Zr}^x]$, which suggest the asumption above holds at

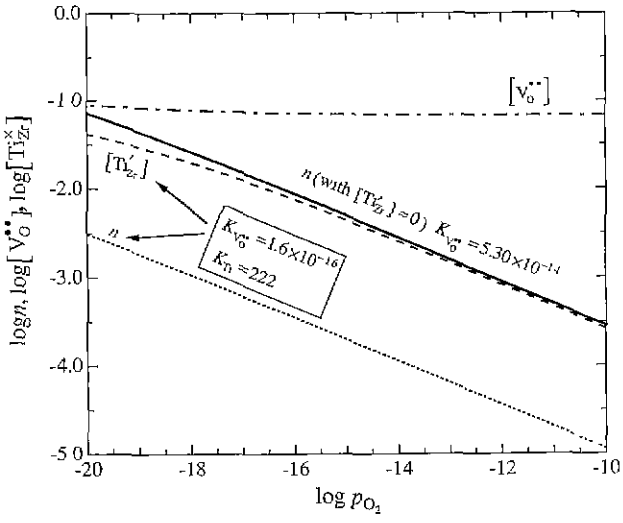

Fig. 9. Calculated concentrations [Vö], n and [Ti'$_{Zr}$] based on the defect models.

reducing conditions and the ratio of [Ti'$_{Zr}$] to [$Ti_{Zr}^{\times}$], can be expressed as follows.

$$\frac{[Ti'_{Zr}]}{[Ti_{Zr}^{\times}]}=\left(\frac{2K_{V_O}K_{Ti}^2}{[Y'_{Zr}]}\right)^{1/2}p_{O_2}^{-1/4} \tag{11}$$

On the other hand, the extent of oxygen nonstoichiometry, δ in TD-YSZ at 1273 K was estimated by measuring the weight change of the samples equilibrated at $p_{O_2}=10^{-18}$ and 0.21, as shown in Table 1. If [Ti'$_{Zr}$] is small, K_{V_O} values can be estimated using the assumption, 2[Vö]≈ [Y'$_{Zr}$]>>n, p. The resultant K_{V_O} exhibits strong dependency on doped Ti ion concentration. For the other situation where [Ti'$_{Zr}$] should be taken into account, K_{Ti} can be estimated assuming that K_{Ti} is independent of Ti concentration. Numerical calculation on eq'ns (5), (7), and (8) with K_{Ti}=222 and $K_{V_O}=1.63\times10^{-14}$, showed good agreement with the nonstoichiometry data, but the Ti^{3+} fraction in the total Ti concentration was almost 1/4, which is much larger than the n values. The variations of n and Vö for 10TD-YSZ are depicted in Fig. 9, together with those evaluated by the model with $K_{V_O}=5.32\times10^{-11}$ and the assumption that [Ti'$_{Zr}$] is negligibly small. It should be noted that n is proportional to -1/4 power of p_{O_2}, if the mobility of electrons is assumed to be independent of their concentration. [Ti'$_{Zr}$] is also proportional to the -1/4 power of p_{O_2} with the exception for the region where [Ti'$_{Zr}$] is almost comparable to [$Ti_{Zr}^{\times}$].

2. *Consistency of the partial and total conductivities*

Since partial conductivities of electrons and holes are approximated to be proportional to $p_{O_2}^{-1/4}$ and $p_{O_2}^{1/4}$, respectively, total conductivity of 10TD-YSZ is given by the following equation,

$$\sigma_t=\sigma_{ion}+\sigma_n^{\circ}p_{O_2}^{-1/4}+\sigma_p^{\circ}p_{O_2}^{1/4}, \tag{12}$$

where σ_v° αvδ σ_p° are the partial conductivities of electrons and holes in equilibrium with p_{O_2}=1.0. In the regime of log $p_{O_2}\leq0$, maximum σ_p value is about $10^{3.5}$ times smaller than the σ_{ion} value as shown in Fig. 4. Therefore, the $\sigma_p^{\circ}p_{O_2}^{1/4}$ term in eq'n (12) can be neglected in the measured range of p_{O_2}, and the eq'n (12) is reduced as

$$\sigma_t=\sigma_{ion}+\sigma_n^{\circ}p_{O_2}^{-1/4}, \tag{13}$$

The relationships between the experimental results of log σ_t and log p_{O_2} by the ac method were fitted to the eq'n (13) with the assumption that σ_{ion} value is independent p_{O_2} and the calculated results are plotted in Fig. 10. From the separate studies on the total conductivity and transference number determination by the concentration cell method, σ_{ion} is suggested as being independent of p_{O_2} and σ_n being proportional to $p_{O_2}^{-1/4}$ between log p_{O_2}= 0 and -20.[13] Also, it is a good approximation for the defect chemical calculation, even though the extent of oxygen nonstoichiometry is as much as those listed in Table 1. The σ_n values calculated from the total conductivity show excellent agreement with those determined by the dc polarization method, but large disagreement can be seen at lower p_{O_2} region.

The σ_n can be also estimated from the results of t_{ion} by the current interruption method together with σ_{ion} data

Table 1. The Extent of Nonstoichiometry, Defined as δ in $Zr_{0.852(1-x)}Y_{0.148(1-x)}Ti_xO_{1.926+0.07x-\delta}$, of TD-YSZ Determined by the Weight Change Between p_{O_2}=0.21 and 10^{-18}

X_{TiO_2}	δ in $Zr_{0.852(1-x)}Y_{0.148(1-x)}Ti_xO_{1.926+0.07x-\delta}$
0.0173	0.0033
0.0534	0.0065
0.0981	0.0129
0.128	0.0154
0.141	0.0182

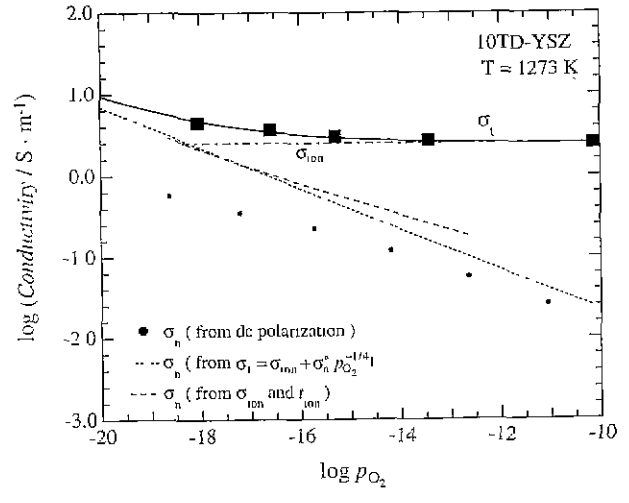

Fig. 10. Comparison between measured and calculated conductivities at 1273 K.

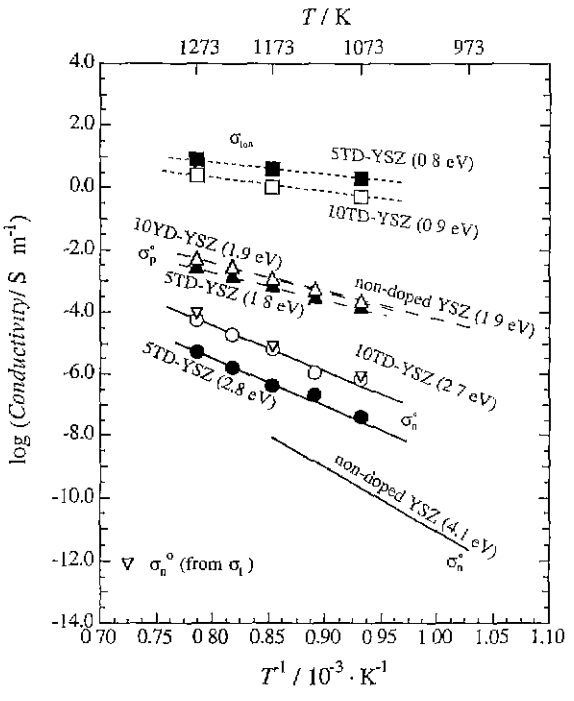

Fig. 11. Arrhenius plots of partial conductivities, σ_{ion}, σ_n, and σ_p for 5 and 10TD-YSZ.

by the total conductivity measurements. The results superimposed in Fig. 10, show good coincidence with σ_n from eq'n (13) other data at higher p_{O_2} regime, but the slope is lower than -1/4.

Arrhenius plots of partial conductivities are summarized in Fig. 11 together with those of 5TD-YSZ. σ_{ion} showed decrease with the increase of Ti concentration, and σ_p° stays almost at the same value or slightly increases. σ_n° values show marked increase with the increase of Ti concentration, which cannot be explained by none of the model described above, if the mobility of electrons are independent of Ti concentration. Another interesting feature is that the apparent activation energy for the partial conductivities are almost the same between 5 and 10TD-YSZ. The activation energy for σ_p° is almost the same with normal YSZ,[14] but that of σ_n° is smaller by 1.3-1.4 eV. The authors suggest the band percolation model for the conduction of electrons, which will be published elsewhere.[15]

All the data except for highly reducing conditions are consistent and show excellent quantitaitive agreement with each other, but significant deviation from -1/4 power law can be seen for σ_n. The deviation is much greater in dc polarization measurements, which is explicitly observed in the Wagner's analysis in Fig. 5. Similar deviation from the prediction by defect chemical model is frequently observed for results by dc polarization measurements in various systems such as YSZ, AgCl, beta-alumina, and so on. Several models are proposed such as the effect of the deviation from Henry's law assumed for dilute defects and the formation of the internal p-n junction.[16] If the former was true, the deviation from the $p_{O_2}^{-1/4}$ dependence should be observed for all the σ_n estimated from different experimental method. To examine the applicability of the latter one, the dc polarization measurements where both electrodes were in the n-type domain, were made. The results are plotted in Fig. 3, where E_{app}s corresponding to $p_{O_2}^{ion}$ are shown by arrows. Excluding the error in very small applied voltage region, the results are consistent with those measured at $p_{O_2}^{ion}$=0.1, suggesting that the inapplicability of the latter model. Another model with the formation of the Schottky barrier is proposed elsewhere.[17]

V. Conclusion

Partial conductivities of electrons, σ_n, and holes, σ_p, in 10TD-YSZ have been measured by the dc polarization method, in addition to the current interruption method for the evaluation of transference number of ions and the total conductivity measurements by the ac impedance method. Except for the partial conductitity of electrons at lower p_{O_2} regime, the partial conductivities of holes, electrons and oxide ions are consistent with the defect chemical model in which the predominant defect is the oxygen vacancy formed for the charge compensation for the substituted Y^{3+} ion on Zr/Ti site.

References

1. W. L. Worell, P. Han, Y. Uchimoto and P. K. Davies, "A New Single Componet Solid Oxide Fule Cell"; pp. 50-57 In Solid Oxide Fuel Cell IV, Proceedings of the 4th Internationsl Symposium on Solid Oxide Fuel Cell (Yokohama, Japan, 1995), Edited by M. Dokiya, O. Yamamoto, H. Tagawa and S C. Singhal. The Electrochemical Society Inc., Pennington, NJ, 1995.
2. H. Naito and H. Arashi, "Electrical Properties of ZrO_2-TiO_2-Y_2O_3", *Solid State Ionics*, **53-56**, 436-441 (1992).
3. T. Lindegaard, C. Clausen and M. Mogensen, "Electrical and Electrochemical Properties of $Zr_{0.77}Y_{0.13}Ti_{0.1}O_{1.93}$"; pp. 311-318 In the 14th Riso International Symposium on Matererials Science, Edited by F. W. Poulsen, J. J. Bentzen, T Jacobsen, E. Skou and M. J. L. Ostergard, 1993.
4. A. Kopp, H Nafe, W. Weppner, P. Kountouros and H. Schubert, "Ionic and Electronic Conductivity of TiO_2-Y_2O_3-Stabilized Tetragonal Zirconia Polycrystals"; pp. 567-575 In Zirconia V, Proceedings of the International Conference on Airconica Science, Edited by S. P. S. Badwal, M. J. Bannister and R. H. J. Hannink, Technomic, Lancaster, PA, 1993.
5. K. Kobayashi, Y. Kai, S. Yamaguchi, N. Fukatsu, T. Kawashima and Y. Iguchi, "Electronic Conductivity Measurements of 5 mol% TiO_2-doped YSZ by a D.C.-Polarization Technique", *Solid State Ionics*, **93**, 193-199 (1997).
6. K. Kobayashi, K. Kato, K Terabe, S. Yamaguchi and Y.

Iguchi, "Metastable Phase Relationship in the ZrO_2-$YO_{1.5}$, ZrO_2-TiO_2 and $YO_{1.5}$-TiO_2 Systems", *J. Ceram, Soc. Jpn*, in press.

7. K. Kobayashi, K. Kato, K. Terabe, S. Yamaguchi and Y. Iguchi, "Total Electrical Conductivity Measurements of TiO_2 Doped YSZ Ceramics", *Submitted to J. Ceram. Soc. Jpn.*
8. Metals HandBook 8th Edition; p1189-1193, Vol. 1, Edited by T. Lyman, H. E. Boyer, P. M. Unterweiser, J. E. Foster, J. P. Hontas and H. Lawton, Am. Soc. Metals, Metals Park. Novelty, Ohio 1961.
9. J. Mizusaki and K. Fueki, "Electrochemical Determination of Electronic Conductivity of AgCl as a Function of Silver Activity", *Revue de Chimie Minerale*, **17**, 356-367 (1980).
10. C. Wagner, "Galvanic Cells with Solid Electrolytes Involving Ionic and Electronic Conduction", pp. 361-377 In Proceeding of the 7th International Confefence on Electrocheminstry, Thermodynamic Kinetics (Linday 1955), Butterworth, London, 1956.
11. K. E. Swider and W. L. Worrell, "Electronic Conduction Mechanism in Yttria-Stabilized Airconia-Titania under Reducing Atmospheres", *J. Electrochem. Soc.*, **143**, 3706-3711 (1996).
12. N. Nicolso, J. Maier, F. K Koschnick and J. M Spaeth, "Local Structure and Oxygen Transport in Transition Metal Doped YSZ", *Radiation Effect and Defects in Solids*, **137**, 259-265 (1995).
13. T. Kawashima, K. Kobayashi and S.Yamaguchi, Unpublished work.
14. W. Weppner, "Electrochemical Transient Investigations of Diffusion and Concentration of Electrons in Yttria Stabilized Zirconia-Solid Electrolyte", *Z. Naturforsch.*, **31a**, 1336-1343 (1976).
15. K. Kobayashi, S. Yamaguchi and Y. Iguchi. "Electronic Transport Properties of TiO_2 Doped YSZ - Dependence of the Electronic Conductivity on TiO_2 Concentration and Band Percolation Model", To be published.
16. W. Weppner, "Tetragonal Zirconia Polycrystals - a High Performance Solid Oxygen Ion Conductor", *Solid State Ionics*, **52**, 15-21 (1992).
17. K. Kobayashi, S. Yamaguchi and Y. Iguchi, "Interfacial Resistivity at Solid Electrolyte/Metal Electrode Interface", To be published in the Proceeding of PacTim 3 (Korea, 1998).